Proceedings World Geothermal Congress 2000
Kyushu - Tohoku, Japan, May 28 - June 10, 2000

VELOCITIES OF CONVECTIVE ASCENDING FLOW IN GEOTHERMAL SYSTEMS BASED ON STATIC TEMPERATURE LOGGING DATA ANALYSIS AND SIMULATION STUDY

Masaji Kato[1], Mineyuki Hanano[2] and Katsuhiko Kaneko[1]
[1]Hokkaido University, Sapporo, Hokkaido 060-8628 Japan
[2]Japan Metals & Co., Ltd., 1-3-6 Saien, Morioka-city, Iwate 020-0024 Japan

Key Words: ascending flow velocity, hydrothermal convection, static temperature log, one-dimensional flow analysis, two-dimensional numerical simulation

ABSTRACT

Macroscopic velocities of convective ascending flow in hydrothermal convection systems show typical characteristics. Our objective is to clarify its characteristics of the systems. In this study, we conducted static temperature logging data analyses and numerical simulation studies. From simple one-dimensional analyses based on static temperature logging data, it was found that the velocities of convective ascending flow in active convection systems had the same order of values. Simulation studies for liquid-dominated hydrothermal systems were also conducted in order to clarify the effects of heat source temperature or permeability structure on the velocities of ascending flow. As a result, in spite of large difference of heat source temperature or permeability structure in a practical range, ascending flow velocity changes only in less than one order of magnitude.

1. INTRODUCTION

Convective ascending flow is an important phenomenon for understanding hydrothermal convection system and therefore for geothermal development. Hydrothermal convection systems have one or more domains of convective ascending flow. In this study, based on static temperature logging data from several geothermal areas, simple one-dimensional analysis for estimating macroscopic velocities of ascending flow in active convection systems was employed. The results may be closely related to the structure of permeability and consequently to the stress condition. Hydrothermal convection can be representative as fluid and heat flows in a porous medium heated from below. Numerical simulation studies for liquid-dominated hydrothermal systems, therefore, were also conducted in order to clarify the effects of the permeability structure or the heat source temperature on the velocities of ascending flow in this study.

2. GOVERNING EQUATIONS

Simple governing equations for fluid flow and energy transport are used in this study. Since liquid-dominated hydrothermal systems in natural state before exploitation are treated here, it is assumed that the flow region is represented by a porous layer, the fluid is single-phase (only water), and mass and heat flow is under the steady state. Accordingly, mass, momentum and energy balance equations of mass and heat flow in a porous medium are as follows (e.g. Donaldson, 1962):

$$\nabla \cdot (\rho_f \boldsymbol{v}) = 0 \tag{1}$$

$$\nabla p - \rho_f \boldsymbol{g} + \frac{\mu}{\boldsymbol{k}} \boldsymbol{v} = 0 \quad \text{(Darcy's equation)} \tag{2}$$

$$c_{pf} \rho_f \boldsymbol{v} \cdot \nabla T = \lambda_m \nabla^2 T \tag{3}$$

where boldface type indicates a vector or a second-order tensor quantity. In the above equations, ρ_f, c_{pf} and μ are the density, the specific heat and the dynamic viscosity of fluid, respectively. $\boldsymbol{v}$ is the Darcian velocity vector of fluid. $\boldsymbol{k}$ is the permeability tensor of the porous medium and λ_m is the isotropic thermal conductivity of the saturated porous medium. $\boldsymbol{g}$ is the gravity vector. T is the equilibrium temperature of saturated porous medium and P is the pressure of saturating fluid.

3. ONE-DIMENSIONAL ANALYSIS FOR VERTICAL FLOW IN RESERVOIR

In liquid-dominated hydrothermal convection, preferred orientation of hot-water flow possibly appears. Dominant vertical ascending flow may exist in the layer just above heat source, such as magma intrusion. While, dominant descending water flow may also occur in the layer. In those cases, one-dimensional analysis of vertical flow can be useful to estimate the vertical flow velocity and the vertical permeability of the layer.

Reducing equation (3), we obtain the differential equation for one-dimensional steady-state flow of heat and fluid through saturated homogeneous porous media (Bredehoeft and Papadopulos, 1965):

$$\frac{\mathrm{d}^2 T}{\mathrm{d}z^2} - \alpha \frac{\mathrm{d}T}{\mathrm{d}z} = 0 \tag{4}$$

where $\alpha = c_{pf} \rho_f v_z / \lambda_m$. v_z is the component of velocity in the z (vertical) direction (positive downward). Solving equation (4) with the condition that $T = T_1$ at $z = z_1$ and $T = T_2$ at $z = z_2$ (z_1 and z_2 are arbitrary if their points are in the layer and $z_1 < z_2$), we can obtain the following equation:

$$\frac{T - T_1}{T_2 - T_1} = \frac{\exp\{\alpha(z - z_1)\} - 1}{\exp\{\alpha(z_2 - z_1)\} - 1} \tag{5}$$

In this equation, if $T_1 = T_0$ at $z_1 = 0$ and $T_2 = T_L$ at $z_2 = L$ (the length of vertical section over which temperature measurements extend) then the solution obtained by Bredehoeft and Papadopulos (1965) appears.

Assuming steady ascending flow in a homogeneous half-infinite porous medium and the boundary conditions that $T = T_0$ at $z = 0$, and $\mathrm{d}T/\mathrm{d}z \to 0$ and $T \to T_r$ as $z \to \infty$ when

solving equation (4), we can obtain the following equation (Turcotte and Schubert, 1982):

$$\frac{T_r - T}{T_r - T_0} = \exp(\alpha z) \tag{6}$$

Though equation (6) is only available to ascending flow, equation (5) is applicable to not only ascending flow but also descending flow. Applications of equation (6) to temperature logging data appear in analyses of the Kakkonda field, Japan in Hanano (1998) and Kajiwara et al. (1993) and of the Mori field, Japan in Sakagawa et al. (1994). In those analyses, the linear relationship of z to $\log(T_r - T)$ in the equation is used.

To know whether the temperature data measured satisfy the steady vertical water flow or not, Plots of temperature gradient versus temperature is available (Mansure and Reiter, 1979). From the equation of total energy flux including convection and conduction terms, the following equation is given:

$$\frac{\mathrm{d}T}{\mathrm{d}z} = \alpha(T - T') - \frac{E}{\lambda_m} \tag{7}$$

where E is the total energy flux in vertical direction and T' is the temperature at which the internal heat energy is taken to be zero. This equation shows that the temperature gradient $\Delta T / \Delta z$ is a linear function of the variable T. Thus, plots of $\Delta T / \Delta z$ versus T yield straight lines when α is constant. In regions of uniform vertical convective flow (α = nonzero constant), the plots show nonhorizontal straight lines. If there is no water movement (α =0), that is, heat conduction only exists, the plots show horizontal straight line. If the $\Delta T / \Delta z$ versus T plot is not linear, discussion on vertical water movement can not be made because of a variety of disturbances such as nonconstant V_z, Water flow within the well bore mentioned by Mansure and Reiter (1979) with referring to Ramey (1962), horizontal flow (Lu and Ge, 1996), and time dependent effects, etc.

Kato et al. (1996) investigated a several of temperature logging data obtained from geothermal areas mainly in Japan. An example of one-dimensional analysis for vertically ascending flow using equation (6) is shown below. The procedure of this method to estimate macroscopic ascending velocity and vertical permeability is stated in Hanano (1998).

Fig. 1 shows the temperature profile obtained from the Okuaizu area (Suda and Yano, 1991). Measured temperature shown as open circles implicates temperature profile type of convective ascending flow region. This can be verified using equation (7). $\Delta T / \Delta z$ versus T plot of the temperature data in Fig. 2 shows a linear relation and negative slope. This means that there exists vertical ascending flow. Fig. 3 shows the application result of the one-dimensional analysis to the temperature logging data shown in Fig. 1. Linear regression line is fitted to the data. As a result, the vertical ascending velocity is macroscopically 1.7×10^{-9} (m/s) and in this case the correlation coefficient, R, is 0.996 where λ_m is 2.0 (W/mK), ρ_f is 891 (kg/m^3), and c_{pf} is 4.39×10^3 (J/kgK) at the intermediate depth. In Fig. 1, solid line shows temperature curve calculated based on the ascending velocity obtained in the one-dimensional analysis.

Results of application of this method to more than ten areas show that the velocities of convective ascending flow in the active upflow region of the hydrothermal convection have the same order of values, 10^{-9} (Kato et al., in prep.). This velocity means approximately 3 cm per year. It may be interesting results for geophysicists and geothermal researchers.

4. TWO-DIMENSIONAL NUMERICAL SIMULATION FOR LIQUID-DOMINATED HYDROTHERMAL CONVECTION SYSTEM

In order to investigate the order of velocities of actively convective ascending flow mentioned in the preceding section, we conducted two-dimensional numerical simulation using a simple model under various conditions. In particular, we considered whether the difference of permeability structures or heat source temperatures affects the ascending flow velocities or not. Some results will be shown below in this section.

Galerkin finite element method (FEM) is used in numerical simulation in two dimensions for understanding behavior of steady-state liquid-dominated hydrothermal convection system. The governing equations used here are shown in the previous section (equations (1) to (3)). These differential equations are transformed to simultaneous linear equations and solved for pressure and temperature (e.g. Hanaoka, 1986). Mercer et al. (1975) and Faust and Mercer (1979) were also referred for the calculation of Galerkin FEM and temperature-dependent properties of rocks and water.

Two-dimensional model for the numerical simulation with hydraulic and thermal boundary conditions is shown in Fig. 4. In consideration of symmetry of the convection, a half region of the convection is used for calculation space as shown in this figure. The reservoir has the size of L in length and H_R in height beneath which the basement rock lies. The height of the basement rock, H_B, is 500 m constant. The boundary conditions are also shown in Fig. 4. At the upper boundary (ground surface), both of temperature and pressure are constant. At the lower boundary, heat source exists at the left corner with the value T_H of temperature. At this boundary away from heat source, the temperature is 150 ^{o}C constant.

The reservoir is treated as a permeable porous layer but the basement rock is less permeable. Permeability structure in the reservoir is assumed as in Fig. 5, which has the characteristics of three kinds of depth-dependence and orthogonal anisotropy, and the aspect ratio of permeability components in x- and z-directions is also depth-dependent in the reservoir. In the figure, "linear type" means that permeability is a linear function of depth. In terms of "cubic type", depth-dependency of permeability was introduced on the basis of "cubic law" in Oda (1986). The relation of depth, z, to one component of permeability, k, is given by

$$k = k_0 \left(1 - \frac{z}{\gamma + z}\right)^3 \tag{8}$$

where k_0 is the permeability at the upper boundary and γ is a constant related to the permeability values at the upper and lower boundaries and the reservoir depth. Superscripts (1 and 2) mean the difference of permeability values at the lower boundary of the reservoir.

Here, some of simulation results of the model having 3 km in height and 6 km in length will be illustrated. For FEM calculation, two-dimensional calculation space was divided into 1344 triangular elements. First, the results for heat source temperature of 300 ^{o}C and permeability structure showing (a) linear type, (b) cubic type and (c) the same cubic type but having different value at the lower boundary, respectively, are illustrated in Fig. 6. Vertical permeability, k_V, at the upper

boundary of all types has the value of 10^{-14} m^2. At the lower boundary of the reservoir, k_V's of (a) and (c) types are the same value of 10^{-16} m^2 but for (b) type k_V is 10^{-15} m^2. The ratio of k_H to k_V at the upper boundary is fixed to 10 but k_H and k_V at the lower boundary of the reservoir have the same value. As shown in the figures (a) and (b), remarkable ascending flows occurred at the left side column, that is, the center of the convection. In the figure (c), however, there exists no predominant upflow and temperature distribution is similar to conductive pattern for heat flow. Since macroscopic velocity is treated in this paper, an average velocity at the center column of convection is important. The average velocities in the figures (a) to (c) are 7.0×10^{-9}, 6.3×10^{-9} and 1.1×10^{-9} m/s, respectively.

Figs. 7 and 8 also show simulation results of the model that is different from Fig. 5 only in terms of heat source temperature of 400 ^{o}C in Fig. 7 and of 500 ^{o}C in Fig. 8. In these figures, (a), (b) and (c) are used in the same way as in Fig. 5. The average velocities in Figs. 7 (a) to (c) are 1.1×10^{-8}, 9.7×10^{-8} and 3.0×10^{-9} m/s, respectively. In terms of Figs. 8 (a) to (c), the average velocities are 1.4×10^{-8}, 1.3×10^{-8} and 5.0×10^{-9} m/s, respectively. In this study, in spite of large difference of heat source temperature, ascending flow velocity changes only in less than one order of magnitude. In terms of permeability structure with values in a practical range, velocity similarly changes in less than one order.

Fig. 9 shows vertical temperature profile obtained as a result of numerical simulation corresponding to Fig. 6 (a). In a horizontal row, Fig. 9 (1) shows the temperature profile at the left side column, that is, the center of convective ascending flow, and finally (12) at the horizontally center position of the figure. As shown in Fig. 9 (1), the upper part of temperature curve indicates ascending flow type although the deeper part of its curve is similar to conductive or descending flow type because of the existence of less permeable basement rock. Furthermore, it is found that the ascending flow region is limited near the center of convection.

Fig. 10 shows vertical distribution of flow velocity components in x- and z-directions. The numbers from (1) to (12) express a horizontal position with the same usage of Fig. 9. As shown in Fig. 10 (1), it is clear that in the center of convective ascending flow region the velocity component in z-direction (vertical) is remarkably dominant compared with x-direction (horizontal) by a few orders of magnitude. Therefore, we can apply one-dimensional analysis mentioned in the preceding section to the convective ascending flow region.

5. CONCLUDING REMARKS

In this study, simple one-dimensional analysis based on static temperature logging data and two-dimensional numerical simulation studies for liquid-dominated hydrothermal systems were conducted in order to clarify the effects of the permeability or the heat source temperature on the velocities of ascending flow. Consequently, macroscopic velocities of convective ascending flow in hydrothermal convection systems show typical characteristics. From simple analyses based on static temperature logging data, it was found that macroscopic velocities of ascending flow in active convection systems are obtained within one order of magnitude. From simulation studies, it is shown that, in spite of difference of heat source temperature or permeability structure in a practical range, ascending flow velocity changes only in less than one order of magnitude.

This study contains a matter of conjecture. We are preparing measured data and results obtained by analyses to clear it up.

ACKNOWLEDGEMENTS

We are grateful to the management of Japan Metals and Chemicals Co., Ltd. and JMC Geothermal Engineering Co., Ltd. for their permission to publish this paper. The comment of Dr. Dave Blackwell, Chair of Technical Program Subcommittee, is also gratefully acknowledged.

REFERENCES

Bredehoeft, J. D. and Papadopulos, I. S. (1965). Rates of vertical groundwater movement estimated from the earth's thermal profile. *Water Resour. Res.*, Vol.1 (2), pp.325-328.

Donaldson, I. G. (1962). Temperature gradients in the upper layers of the earth's crust due to convective water flows. *J. Geophys. Res.*, Vol.67 (9), pp.3449-3459.

Faust, C. R. and Mercer, J. W. (1979). Geothermal reservoir simulation 1. Mathematical models for liquid- and vapor-dominated hydrothermal systems. *Water Resour. Res.*, Vol.15 (1), pp.23-30.

Hanano, M. (1998). A simple model of a two-layered high-temperature liquid-dominated geothermal reservoir as a part of a large-scale hydrothermal convection system. *Transport in Porous Media*, Vol.33 (1), 3-27.

Hanaoka, N. (1986). Structural control of hydrothermal system by gravity basement. *J. Geothermal Res. Soc. Japan*, Vol.8 (4), pp.379-412. (in Japanese with English abstract)

Kajiwara, T., Hanano, M., Ikeuchi, K., and Sakagawa, Y. (1993). Permeability structure at the Kakkonda geothermal field, Iwate Prefecture, Japan. *Abstracts with Programs*, *1993 Annual Meeting, Geothermal Res. Soc. Japan, Tokyo*, B30. (in Japanese)

Kato, M., Kaneko, K. and Hanano, M. (1999): Velocities of convective ascending flow in liquid-dominated hydrothermal convection systems, *Proc. 24th Workshop on Geothermal Reservoir Engineering, Stanford University, Stanford*, pp.164-167

Kato, M., Kawakami, Y., Hanano, M., and Tominaga, Y. (1996). Velocities of convective ascending flow in several geothermal fields –Analyses based on static temperature logging data–. *Abstracts with Programs*, *1996 Annual Meeting, Geothermal Res. Soc. Japan, Tokyo*, A33. (in Japanese)

Lu, N. and Ge, S. (1996). Effect of horizontal heat and fluid flow on the vertical temperature distribution in a semiconfining layer. *Water Resour. Res.*, Vol.32 (5), pp.1449-1453.

Mansure, A. J. and Reiter, M. (1979). A vertical groundwater movement correction for heat flow. *J. Geophys. Res.*, Vol.84 (B7), pp.3490-3496.

Mercer, J. W., Pinder, G. F., and Donaldson, I. G. (1975). A Galerkin-finite element analysis of the hydrothermal system at Wairakei, New Zealand. *J. Geophys. Res.*, Vol.80 (17), pp.2608-2621.

Ramey, Jr., H. J. (1962). Wellbore heat transmission. *J. Petrol. Technol.*, Vol.14, pp.427-435.

Oda, M. (1986): An equivalent continuum model for coupled stress and fluid flow analysis in jointed rock masses, *Water Resour. Res.*, Vol.22 (13), pp.1845-1856

Sakagawa, Y., Takahashi, M., Hanano, M., Ishido, T., and Demboya, N. (1994). Numerical simulation of the Mori geothermal field, Japan. *Proc. 19th Workshop on Geothermal Reservoir Engineering, Stanford University, Stanford*, pp.171-178.

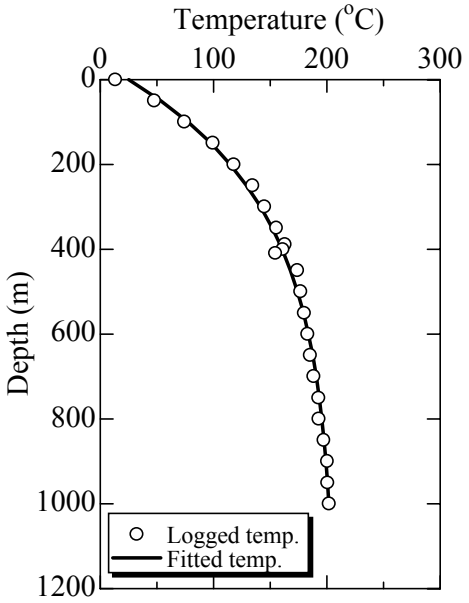

Fig. 1 Temperature profiles at N58-OA-7 well in the Okuaizu area. Measured temperature data is from Suda and Yano (1991). Solid line shows temperature profile fitted based on the ascending velocity obtained.

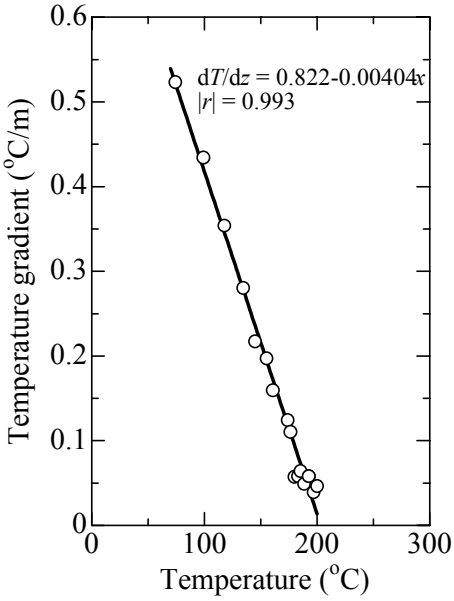

Fig. 2 Temperature gradient versus temperature plot of data in Fig. 1.

Suda, Y. and Yano, Y. (Eds.) (1991). Well data compiled from Japanese nation-wide geothermal surveys, part 2 logging data and geologic columns data. *Rept Geol. Surv. Japan*, No.273, 842pp. (in Japanese with English abstract)

Turcotte, D. L. and Schubert, G. (1982). *Geodynamics: Applications of Continuum Physics to Geological Problems*. John Wiley & Sons, New York, 450pp.

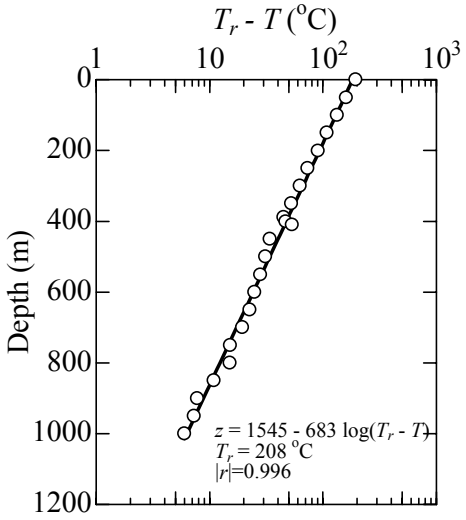

Fig. 3 Fitting result to temperature data in Fig. 1. Solid line shows linear regression line of log (T_r - T) to depth z.

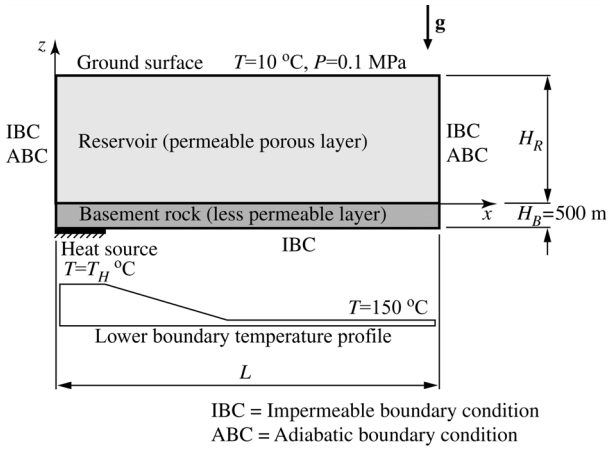

Fig. 4 Two-dimensional model for numerical simulation with boundary conditions.

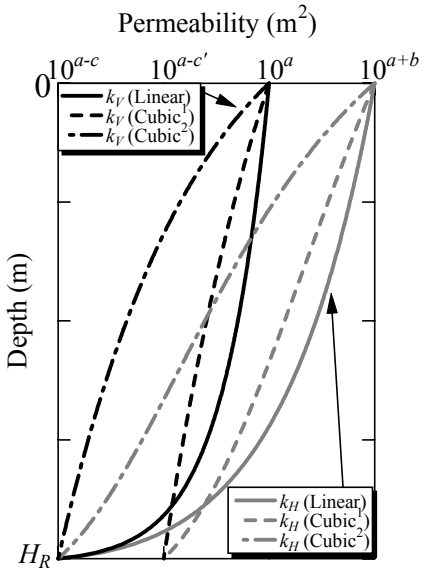

Fig. 5 Permeability structure in the reservoir illustrated in Fig. 4. Permeability is assumed to be depth-dependent and orthogonally anisotropic. The aspect ratio of permeability components in horizontal and vertical directions is also depth-dependent in the reservoir. k_H and k_V denote horizontal and vertical permeability, respectively.

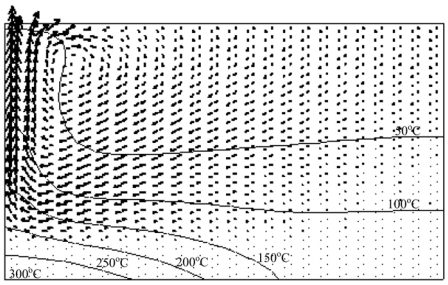

(a) Linear type

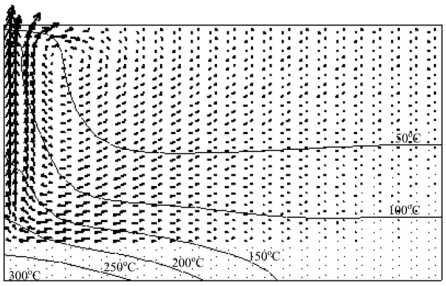

(b) Cubic[1] type

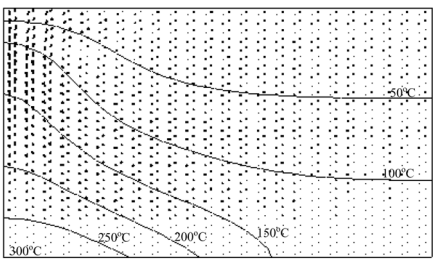

(c) Cubic[2] type

Fig. 6 Simulation results of the model having 3 km in height, 6 km in length, heat source temperature of 300 °C, and permeability structure showing respectively (a) linear type, (b) cubic type and (c) the same cubic type but having different value at lower boundary (see Fig. 5). Maximum length of vectors in these figures is 8.4×10^{-9} m/s.

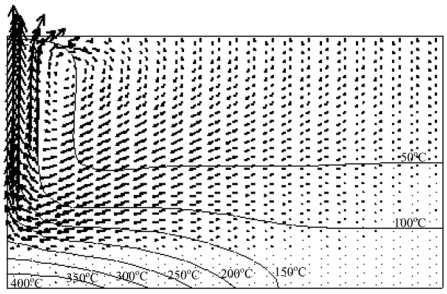

(a) Linear type

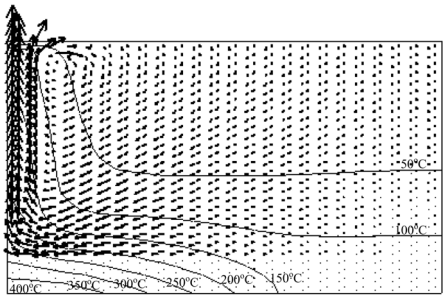

(b) Cubic[1] type

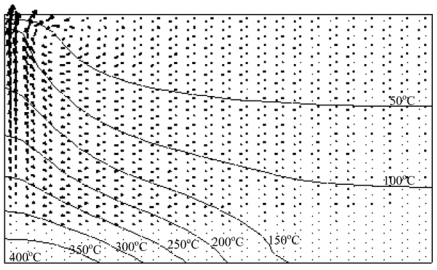

(c) Cubic[2] type

Fig. 7 Simulation results of the model that is different from Fig. 6 only in terms of heat source temperature of 400 °C and (a), (b) and (c) are used in the same way. Maximum length of vectors in three figures is 1.2×10^{-8} m/s.

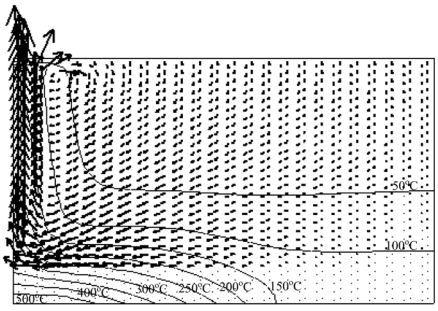

(a) Linear type

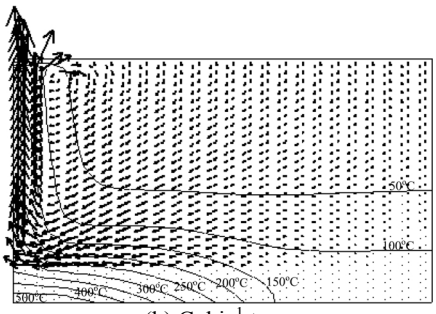

(b) Cubic[1] type

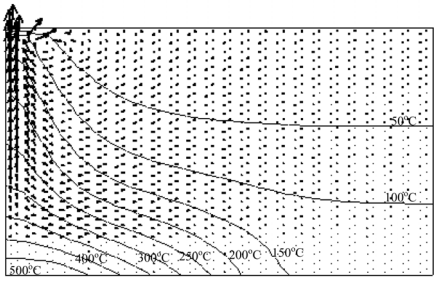

(c) Cubic[2] type

Fig. 8 Simulation results of the model that is different from Figs. 6 and 7 only in terms of heat source temperature of 500 °C and (a), (b) and (c) are used in the same way. Maximum length of vectors is 17 × 10^{-9} m/s.

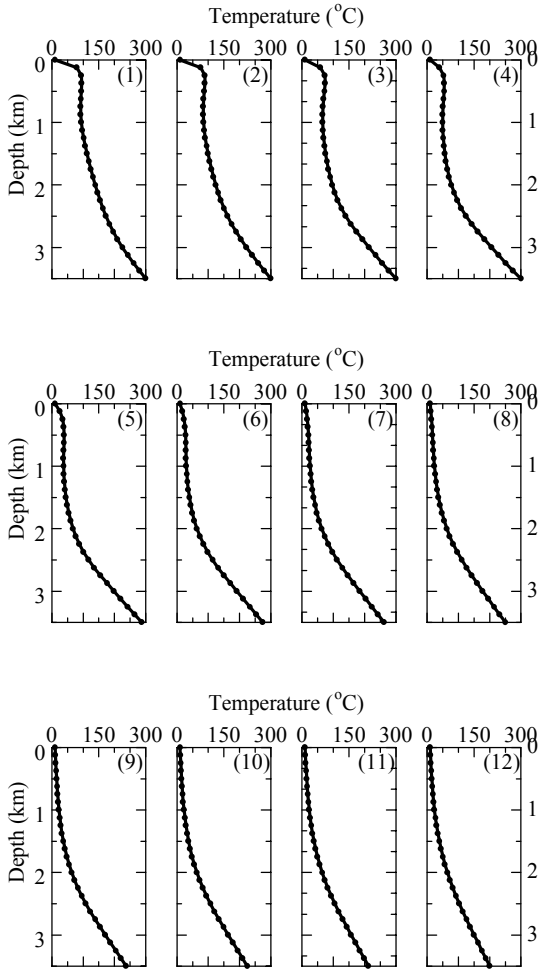

Fig. 9 Vertical temperature profile obtained as a result of numerical simulation corresponding to Fig. 6 (a). In a horizontal row, (1) shows the temperature profile at the left side column, that is, the center of convective ascending flow, and finally (12) at the horizontally center position of the reservoir.

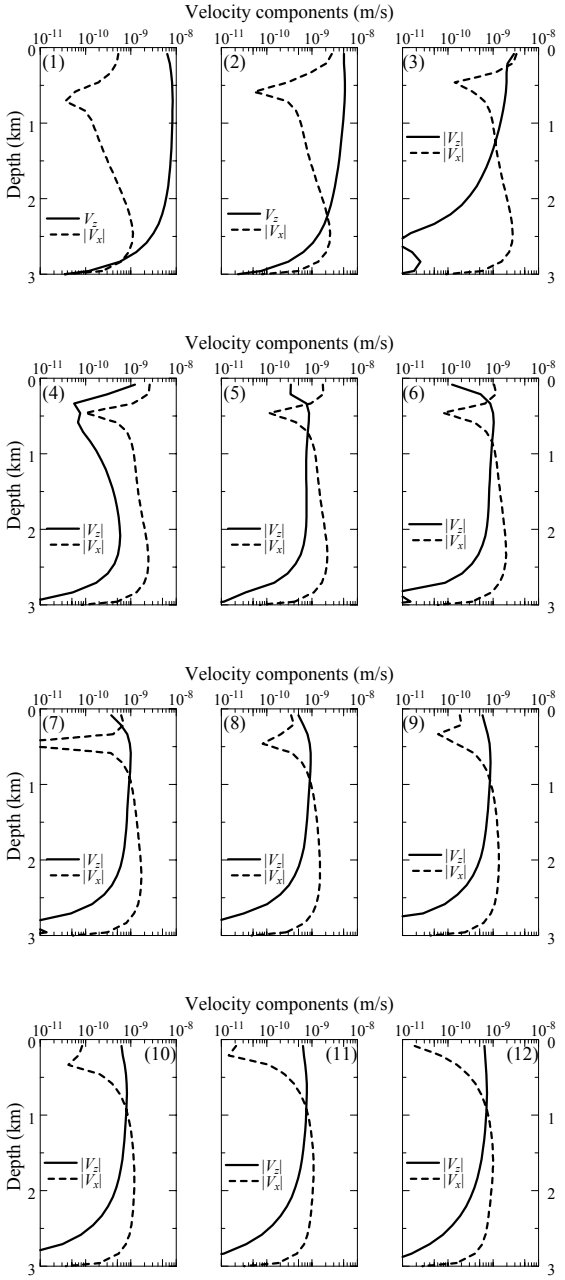

Fig. 10 Vertical distribution of flow velocity components in *x*- and *z*-directions. The numbers from (1) to (12) express horizontal position with the same usage of Fig. 9.